Cryogenics 50 (2010) 647–652

Contents lists available at ScienceDirect

Cryogenics

journal homepage: www.elsevier.com/locate/cryogenics

Thermal characterisation of a tungsten magnetoresistive heat switch

J. Bartlett, G. Hardy, I. Hepburn, R. Ray, S. Weatherstone *

Mullard Space Science Laboratory, UCL, Holmbury St. Mary, Dorking, Surrey RH5 6NT, UK

ARTICLE INFO

Article history:
Received 24 June 2009
Received in revised form 15 February 2010
Accepted 22 February 2010

Keywords:
Magnetoresistance (C)
Thermal conductivity (C)
Adiabatic demagnetisation (E)
Space cryogenics (F)

ABSTRACT

A magnetoresistive heat switch has been developed to improve the performance of our flight-worthy cryogen-free ADR. We have characterised the switch's thermal conductivity in the temperature range 0.3–4 K under an applied magnetic field of 1.8 T for two tungsten samples of different purity. The results are discussed relating to the key aspects of semi-classical magnetoresistance theory. We show that crystal purity has a strong effect on switch performance and magnetoresistive effect. Our findings are verified by comparison to results obtained by other authors. The measured switching ratio for our best sample is 1.75×10^4 at 1.5 K and 1.51×10^4 at 4.26 K. The lattice conductivity remains dominated by the electronic conductivity in the investigated range of temperatures under an applied magnetic field of 1.8 T. In order for the lattice conductivity to dominate a purity of >99.999% would be required.

1. Introduction

Many cryogenic systems require heat flow to be controlled. Heat switches provide this control, allowing thermal isolation and connection between different system components. An 'ideal' heat switch would provide complete thermal isolation in its 'off' state and a strong thermal link in its 'on' state. Complete isolation can only be achieved using mechanical heat switches, which are undesirable for use in space due to the potential for failure.

There has been considerable interest in the concept of exploiting thermal magnetoresistance to form the basis of a heat switch especially for use in adiabatic demagnetisation refrigerators due to the high switching ratio (ratio of 'on' conductance to 'off' conductance). In the space worthy ADR developed at the Mullard Space Science laboratory the low temperature performance is limited by the heat switches used. As shown in [1] replacement with magnetoresistive heat switches offers considerable improvement in performance thereby justifying the slight increase in mass associated with the additional magnet needed. Magnetoresistance is a phenomenon that occurs markedly in compensated metals with closed Fermi surfaces, and is simply a large change in electrical resistance under the application of a sufficiently strong magnetic field. Since the electrical resistance in metals can be related to the thermal resistance (via the Wiedemann–Franz law), an applied magnetic field also changes the thermal conductivity. For tungsten it has been shown [2] that a change in thermal conductivity in the region of 10^4 at 4 K is obtained with magnetic fields in the region of 2–3 T. This allows the possibility of a solid state heat switch with a large switching ratio and where the switching time is limited only by the time taken to magnetise or demagnetise the magnet.

We have measured the thermal conductivity of a tungsten magnetoresistive heat switch over the temperature range 0.3–4 K under an applied magnetic field of 1.8 T for two samples of different purity. In order to identify the relative phonon and electron contributions to the thermal conductivity and the temperature dependency we compare our results to theory.

2. Theoretical treatment of magnetoresistive thermal conductivity

In metals, heat is transported by phonon propagation and free electron diffusion. In the liquid helium regime, the electron diffusion mechanism strongly dominates the thermal conductivity, typically carrying several orders of magnitude more heat per unit time when compared to the phonon mechanism [3]. In zero applied magnetic field, the low temperature thermal conductivity k is a sum of the two contributing mechanisms,

$$k(T) = k_g(T) + k_e(T) \tag{1}$$

where k_gT is the phonon conductivity term and k_eT the electronic conductivity term where both are functions of temperature (T). Compensated metals with a closed Fermi surface are known to exhibit a large thermal magnetoresistive effect. Metals meeting these criteria include Ga, Cd, Be, Zn, Mo and W [3]. Magnetoresistive effect will refer to the thermal magnetoresistive effect only for the rest of this paper.

The origin of the magnetoresistive effect arises from the action of the Lorentz force upon the electrons within the metal when an external magnetic field is applied. The electrons describe curved

* Corresponding author. Fax: +44 (0) 1483 278312.
E-mail address: saw@mssl.ucl.ac.uk (S. Weatherstone).

0011-2275/$ - see front matter © 2010 Elsevier Ltd. All rights reserved.
doi:10.1016/j.cryogenics.2010.02.027

paths under such conditions, manifested as helical orbits in the plane normal to the applied magnetic field. If the magnetic field is strong enough to significantly curve an electron's trajectory within a mean free path, it is likely magnetoresistance will be observed [4]. Electrons describe such orbits on surfaces of constant energy in k-space, e.g. on sheets of the Fermi surface, and have corresponding real space orbits [4]. The frequency of the orbit is the cyclotron frequency, $\omega_c = eB/m^*$, where e is the electronic charge, B is the applied magnetic field, and m^* is the effective electron mass. Since the electrons are locked into these orbits, they diffuse through the metal along a temperature gradient at a greatly reduced rate. As electron diffusion is the dominant process contributing to thermal conductivity, the thermal conductivity is significantly reduced. For the metals Ga, Cd, Be, Zn, Mo and W with a sufficiently high magnetic field, the electron thermal conductivity can be reduced so that phonon conductivity becomes the dominant heat transfer [3].

Magnetoresistive heat switch applications have been investigated for Ga [5], Cd [6], Be [7] and W [3,8]. At sufficiently low temperature these metals all become superconducting. In order for a magnetoresistive heat switch to maintain a useful switching ratio, it needs to be operated above its superconducting transition temperature, T_c. For applications involving milli-Kelvin temperatures, only beryllium and tungsten have a sufficiently low T_c, at 0.026 K and 0.015 K, respectively. To ensure minimal heat conduction in the thermal 'off' state (i.e. the low thermally conducting state achieved with a magnetic field), a metal with a low phonon conductivity must be chosen. A higher Debye temperature, θ_D, implies a lower phonon thermal conductivity. Beryllium has a θ_D of 1000 K, whereas Tungsten has a θ_D of 310 K. Thus, beryllium is clearly an excellent candidate, as Radebaugh's results indicate [7]; however, large single crystals are difficult to obtain and beryllium is highly toxic. Given the present problems in obtaining beryllium, tungsten is the best second choice.

Tungsten has a body-centred cubic (bcc) lattice structure. Following the theoretical approaches taken by Canavan et al. [3], Long [9] and Wagner [10] we summarize the key aspects of the theory for comparison to our thermal conductivity measurements. For an applied magnetic field aligned along an axis of high symmetry within the tungsten crystal, the thermal conductivity tensor simplifies to:

$$k = \begin{pmatrix} k_{xx} & k_{xy} & 0 \\ -k_{xy} & k_{xx} & 0 \\ 0 & 0 & k_{zz} \end{pmatrix} \tag{2}$$

where the applied field is aligned in the z direction and the thermal gradient is along the x direction. The z component of the thermal conductivity does not contribute to heat flow in the orthogonal x–y plane, reducing the effective tensor to a 2×2. The transverse thermal conductivity k_{xy} has been determined by Long [9] to be only a few percent of k_{xx} in the investigated range of temperatures and fields. Thus, it is reasonable to neglect the effects of k_{xy} and assume the thermal conductivity is isotropic within the x–y plane.

Semi-classical magnetoresistance theory shows that compensated metals have a magnetoresistive effect that has a quadratic dependence on applied magnetic field [4,9,10]. Wagner [10], Long [9], and Batdalov [2] find that for high magnetic fields, k_{xx} has the form:

$$K_{xx} = k_g(T) + \frac{A_{xx}(T)}{B^2} \tag{3}$$

where the lattice conductivity $k_g(T)$ is assumed to be completely independent of magnetic field, B is the applied magnetic field and $A_{xx}(T)$ represents the magnetoresistive electronic thermal conductivity. For high fields, Wagner [10] found $A_{xx}(T)$ to be of the form $\frac{A_{xx}(T)}{T} = \alpha_0 + \alpha_3 T^3$, where α_0 and α_3 are constant coefficients.

The high field criterion is given by $\omega_c\tau \gg 1$ [4,9,10], where τ is the electronic relaxation time. $\omega_c\tau$, the mean angle turned between collisions [4], is a difficult quantity to calculate as it requires knowledge of the electron effective mass (m^*) which is a variable quantity. However, we can obtain an estimation of $\omega_c\tau$ by considering the cyclotron frequency definition (shown above) and the electrical conductivity. In the absence of a magnetic field the electrical conductivity, α_0, is given by $\sigma_0 = ne^2\tau/m^*$, where n is the electronic number density. By combining this with the cyclotron frequency definition we obtain

$$\omega_c\tau = \frac{B\sigma_0}{ne} \tag{4}$$

The thermal conductivity k may be related to the electrical conductivity via the Wiedemann–Franz law (Eq. (5)) if inelastic scattering between electrons and phonons may be neglected [11], i.e. at not too low temperatures (whilst the electron momentum dissipation path length remains equal to the electron energy dissipation path length) and high temperatures (significantly above the Debye temperature):

$$\frac{k}{\sigma_0} = L_0 T \tag{5}$$

where L_0 is the Lorenz number derived from free-electron theory and has the theoretical value $L_0 = 2.44 \times 10^{-8}\ \mathrm{W\,\Omega\,K^{-2}}$. Long [12] shows that in the 1–4 K region the Lorenz number increases from L_0 with increasing temperature to a value of $\sim 4 \times 10^{-8}\ \mathrm{W\,\Omega\,K^{-2}}$ at 4 K. Wagner et al. [13] show that the Lorenz number decreases from L_0 with increasing temperature within the same temperature region as Long, but with variations between different samples of Tungsten. Wagner et al.'s value of the Lorenz number varies between $\sim 1.2 \times 10^{-8}\ \mathrm{W\,\Omega\,K^{-2}}$ and $\sim 2.2 \times 10^{-8}\ \mathrm{W\,\Omega\,K^{-2}}$ at 4 K. Noting the difference between the experimentally measured results of these authors, we assume the Wiedemann–Franz law makes a reasonable approximation to the Lorenz number for Tungsten. We use our measured zero magnetic field thermal conductivity ($48.27\ \mathrm{kW\,m^{-1}\,K^{-1}}$ at 4.26 K for sample 1) to determine σ_0, and find $\sigma_0 = 4.64 \times 10^{11}\ \Omega^{-1}\,\mathrm{m}^{-1}$. Assuming two conduction electrons per atom [14], the electron number density, n, will be $1.26 \times 10^{29}\ \mathrm{m}^{-3}$. Using Eq. (4) we find $\omega_c\tau = 23B$ for sample 1. For an applied field of 1.8 T we have a value of 41 for $\omega_c\tau$ for this sample. The requirement for the high magnetic field case is that $\omega_c\tau$ is much greater than 1. We will consider that a value of 41 satisfies this criterion.

The temperature dependency of the phonon conductivity component k_gT is dependent upon the nature of the scattering mechanisms present. If the phonon current is limited by scattering of conduction electrons or dislocations, we would expect a T^2 relationship; whereas if it is limited by boundary scattering then a T^3 relationship would be expected [12]. In the analysis of our measurements we will consider both cases. We thus fit our thermal conductivity data to the equation:

$$k_{xx} = PT^u + \frac{A_{xx}(T)}{B^2} \tag{6}$$

where P is the phonon conductivity coefficient, u will be either 2 or 3 and $A_{xx}(T)$ is the high magnetic field electronic conductivity term which has the form $\frac{A_{xx}}{T} = \alpha_0 + \alpha_3 T^3$. Long [12] suggests that boundary scattering is not significant for his sample, and thus expects the phonon conductivity to have a T^2 form.

3. Experimental

Two samples of different purity single crystal Tungsten were used for the characterisation of the thermal conductivity.

Photographs of the samples are shown in Fig. 1. The geometry of the samples were based on a design permitting a long path length yet preserving a small physical size, as shown in Canavan et al. [3]. The key dimensions of the thermal path are a square cross section A of 1.5 mm × 1.5 mm and an effective path length of L = 0.43 m. The purity of sample 1 has been measured to be 99.999% and that of sample 2 to be 99.992%. Both samples were grown and wire-electronic discharge machined by Mateck GmbH [15]. Purity analyses were performed using GDMS (Glow Discharge mass-spectrometry), and the full results are presented in Table 1. The thermal conductivity experiments were carried out in a laboratory cryostat containing an ADR cooled by a liquid helium bath.

Sample 1 was vacuum brazed onto two copper arms (one per end of the tungsten crystal) in order to be able to mount the sample for testing. For sample 2 the mounting flanges were an integral part of the crystal as can be seen in Fig. 1b. In order to measure the thermal conductivity one of the arms was bolted to the cold finger of the ADR while the other was left free. The magnetic field for the tungsten samples was generated by a magnet surrounding the cold finger of the ADR, capable of providing a magnetic field of up to 1.8 T. In order for the vacuum brazed joint of sample 1 to not influence the measurements the thermometers and heater were mounted on one layer of the tungsten giving an effective path length of L = 9.4 mm. In order to minimise any radiation heat load from higher temperature stages (4 K), a dual-layer Mylar radiation shield was used to enclose the crystal and its support structure.

Power was applied to a heater (10 kΩ metal film resistor) to create a small but measureable temperature difference (ΔT) of 0.1 K between the two ends for different base temperatures set by the ADR. For each measurement, the base temperature (cold end) was set by manually magnetising/demagnetising the ADR until the desired temperature was achieved. Once the cold end was at the desired temperature, the system was left to achieve thermal equilibrium, so as to ensure that the initial conditions saw the two ends of the crystal at the same temperature, i.e. no temperature gradient with zero applied power. Current was then supplied to the heater. The input power was measured by monitoring the supplied current and the voltage across the 10 kΩ resistor. The applied heater power is then simply equal to the product of these quantities. For each measurement, the power was gradually increased by increasing supply current, until a sufficient temperature gradient was achieved between the two crystal ends. Once such a temperature gradient was established, the equilibrium temperatures were recorded. The applied power was then removed and the thermometer resistances recorded as the tungsten cooled back thus ensuring that the previous initial conditions were still valid and no change had occurred.

Table 1
Full results of GDMS (gas discharge mass-spectrometry) purity analyses for samples 1 and 2. Elemental concentrations are by mass in μg/g.

Element	Sample 1	Sample 2	Element	Sample 1	Sample 2
Ag	<0.004	<0.005	N	<0.01	<0.01
Al	0.02	0.05	Na	0.10	0.06
As	<0.004	<0.008	Nb	0.04	0.2
Au	<0.009	<0.009	Nd	<0.002	<0.002
B	<0.001	<0.002	Ni	<0.006	<0.009
Ba	<0.002	<0.002	O	<0.7	<0.5
Be	<0.0006	<0.0008	Os	<0.07	<0.07
Bi	<0.004	<0.005	P	<0.003	<0.004
Br	<0.005	<0.004	Pb	<0.006	0.03
C	<2.7	<3.7	Pd	<0.002	<0.002
Ca	0.04	<0.01	Pr	<0.0003	<0.0004
Cd	<0.02	<0.03	Pt	<0.003	<0.003
Ce	<0.0008	<0.001	Rb	<0.0005	<0.0007
Cl	<0.009	<0.004	Re	<0.08	<0.09
Co	<0.001	0.01	Rh	<0.0009	<0.003
Cr	0.02	0.05	Ru	0.00	<0.004
Cs	<0.06	<0.03	S	0.06	0.04
Cu	6.1	2.7	Sb	<0.009	<0.01
Dy	<0.001	<0.002	Sc	<0.0001	<0.0002
Er	<0.0009	<0.001	Se	<0.02	<0.02
Eu	0.08	0.1	Si	0.20	0.08
F	<0.003	<0.01	Sm	0.00	0.01
Fe	0.04	0.2	Sn	<0.03	<0.04
Ga	0.01	<0.009	Sr	0.00	<0.0004
Gd	<0.002	<0.002	Ta	<1.8	<22
Ge	<0.08	<0.09	Tb	<0.0003	<0.0004
Hf	<0.01	<0.01	Te	<0.009	<0.01
Hg	<0.05	0.9	Th	<0.0004	<0.0002
Ho	<0.0003	<0.0005	Ti	<0.0006	0.01
I	<0.0004	<0.0005	Tl	<0.0005	<0.0008
In	0.01	<0.005	Tm	<0.0004	<0.0005
Ir	O.0007	0.02	U	<0.0003	<0.0004
K	<0.03	<0.09	V	<0.0005	0.01
La	<0.0007	<0.0009	W	Matrix	Matrix
Li	0.00	<0.001	Y	<0.0002	0.001
Lu	<0.0003	<0.0005	Yb	<0.001	<0.002
Mg	0.01	0.08	Zn	0.06	0.5
Mn	0.00	<0.002	Zr	<0.002	<0.002
Mo	0.60	50			
			Total	9.3 μg/g	77.2 μg/g

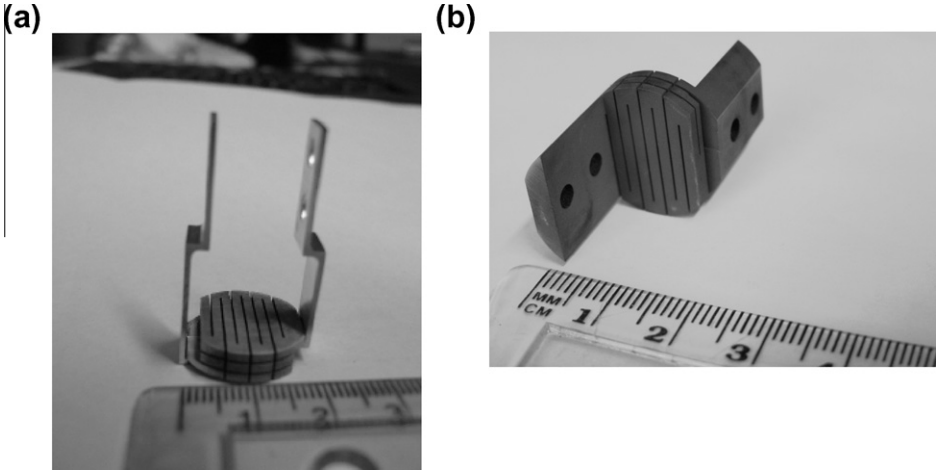

Fig. 1. The tungsten magnetoresistive heat switch. MSSL tungsten heat switch samples. Fig. 1a (Left) shows sample 1. Copper arms are vacuum brazed to the tungsten in order to mount the sample during measurement. Fig. 1b (Right) shows sample 2, with integral mounting support arms.

The temperature measurements were made using Cernox resistance thermometers (which are insensitive to magnetic fields) and an AVS 47 resistance bridge. Thus, for each measurement, the raw data consists of the supplied heater power $\dot{Q}$ and the equilibrium resistances of the hot and cold end thermometers. The resistances are converted to temperature using the thermometer manufacturer's supplied calibration data and a polynomial fit to this calibration data. The thermal conductivity is then simply calculated using Eq. (7):

$$k(T) = \frac{L}{A}\left(\frac{\dot{Q}}{\Delta T}\right) \tag{7}$$

where ΔT is the average temperature between the hot and cold thermometers; L and A retain their previous definitions.

4. Experimental results and analysis

The measured thermal conductivity for sample 1 (the higher purity sample) is shown in Fig. 2 for both the 'on' and 'off' states, where the 'on' state refers to zero applied magnetic field (high thermal conductivity) and the 'off' state refers to an applied 1.8 T magnetic field, hence a low thermal conductivity. Due to the high thermal conductivity in the 'on' state we have only been able to measure it at 1.5 and 4.2 K, the temperatures obtained with our liquid helium bath. We find that the 'on' thermal conductivity of sample 1 is 48.3 kW m^{-1} K^{-1} at 4.26 K, and 14.4 kW m^{-1} K^{-1} at 1.50 K. Fig. 3 shows more clearly the measured 'off' thermal conductivity values presented in Fig. 2, along with the measured 'off' state conductivity for sample 2. The apparent scatter in the data at the high end of the investigated temperature range is a result of measurement uncertainty due to the lower measurement resolution associated with the thermometry at higher temperatures.

We fit the data shown in Fig. 3 with Eq. (6) for the following scenarios for sample 1:

(1) No phonon contribution to the thermal conductivity.
(2) A T^3 phonon conductivity dependence.
(3) A T^2 phonon conductivity dependence.

As can be seen from Fig. 3, a fit with no phonon contribution fits the sample 1 data well indicating that the phonon contribution to the thermal conductivity for this sample may be low in this temperature range at an applied magnetic field of 1.8 T. Fits to the data with the T^3 and T^2 phonon relationship are identical and fit our data better. However, we cannot distinguish whether the phonon contribution follows a T^3 or T^2 form and thus use the assumption of Long [12], i.e. a T^2 relationship.

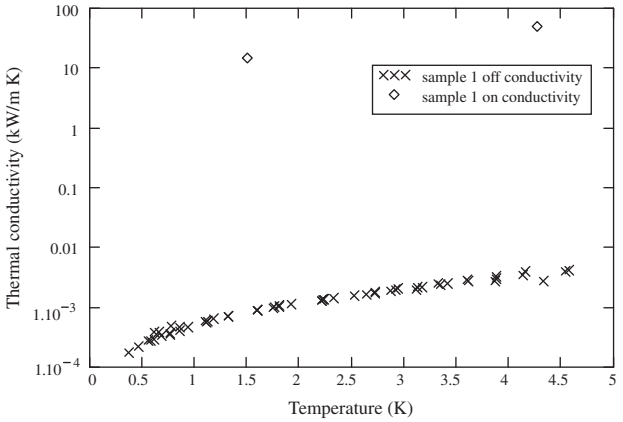

Fig. 2. Measured sample 1 thermal conductivity in 'on' (zero field) and 'off' (1.8 T field) switch states. Measured sample 1 thermal conductivity as function of temperature for zero applied field 'on' state (diamonds) and 1.8 T applied field 'off' state (x's).

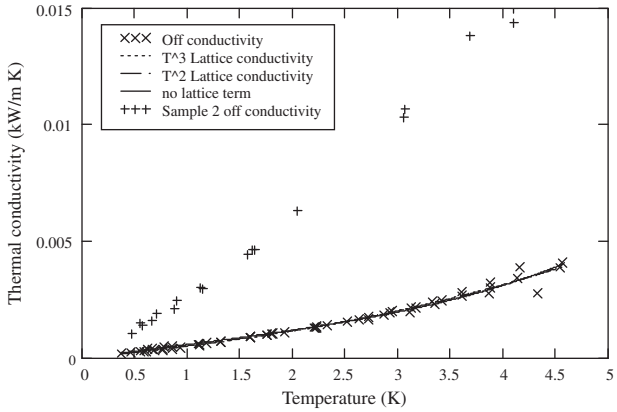

Fig. 3. Measured 'off' conductivity for samples 1 and 2. Measured thermal conductivity under 1.8 T applied field 'off' state plotted as a function of temperature for sample 1 (x's) and sample 2 (crosses). Sample 1 data is fit to Eq. (6) assuming: (1) No lattice contribution to the thermal conductivity (solid line), (2) a T^3 dependent lattice conductivity (dotted line) and 3) a T^2 dependent lattice conductivity (dashed line). The lines for scenario (2) and (3) directly overlap.

Assuming a phonon relationship of T^2 we can obtain from our fit to the data values for P, α_0 and α_3. These are presented in Table 2 along with published values.

Fig. 3 shows very clearly that the measured 'off' state conductivity of sample 2 is much higher than that of sample 1. The lower purity of sample 2 is a highly plausible explanation for this sample's poor performance. Clearly purity has a very strong influence on magnetoresistive effect; the steeper gradient of the sample 2 thermal conductivity data suggests the electron contribution to the thermal conductivity is significantly higher than for sample 1. Attempting to fit the sample 2 data to high field theory yields unphysical negative values for the parameter α_3. This indicates that 1.8 T is insufficient to push sample 2 into the high field regime.

4.1. Comparison of thermal conductivity to results from the literature

Measurements of the total thermal conductivity of tungsten under an applied magnetic field have been made by Batdalov and Red'ko [2], Duval et al. [8] and Canavan et al. [3]. Fig. 4 shows our measured data in comparison to the work of these authors under similar conditions to our measurements. It appears that our sample 1 measured thermal conductivity under an applied field of 1.8 T correlates well with Duval et al.'s [8] measured thermal conductivity under an applied field of 3 T. Duval et al. point out the 3 T magnetic field was inhomogeneous along the length of their sample; hence the effective field will likely be lower than 3 T. Canavan et al.'s [3] data provides us with only two relevant

Table 2
Table comparing calculated coefficients in Eq. (6) to published values. Comparison of calculated fit parameters for sample 1 to published values.

Parameter	Wagner[a]	Long	Canavan	Our sample
P	0.050 W m^{-1} K^{-3}	0.037 W m^{-1} K^{-3}	–	0.066 T^2 W m^{-1} K^{-3}
μ	2	2	–	2
α_0	0.42 T^2 W m^{-1} K^{-2}	–	1.37 W T$^{1.7}$ m^{-1} K^{-2}	1.4 T^2 W m^{-1} K^{-2}
α_3	0.0063 T^2 W m^{-1} K^{-5}	–	0.0061 T^2 W m^{-1} K^{-5}	0.0040 T^2 W m^{-1} K^{-5}

[a] Calculated by Canavan et al.

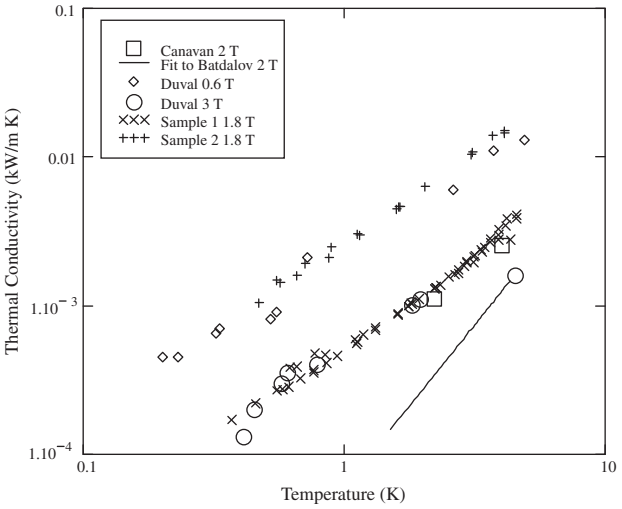

Fig. 4. Comparison of measured 'off' state conductivities to published results from similar investigations. Measured thermal conductivity under 1.8 T applied field 'off' state as function of temperature for sample 1 (x's) and sample 2 (crosses). Plotted alongside a fit to Batdalov and Red'kos measured thermal conductivity under an applied field of 2 T (solid line), Duval et. al.'s measured thermal conductivity under an applied field of 0.6 T (diamonds) and 3 T (circles) and Canavan et. al.'s measured thermal conductivity under an applied field of 2 T (squares).

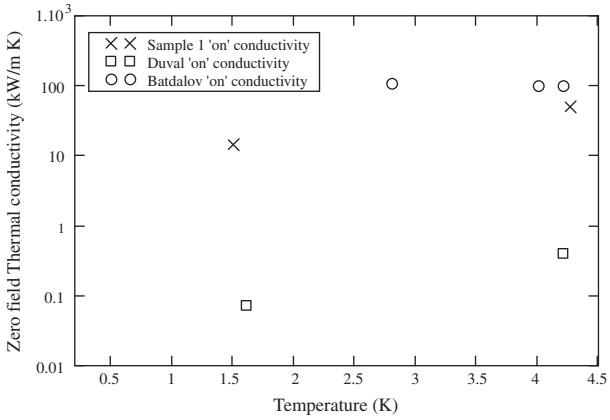

Fig. 5. Measured thermal conductivity of sample 1 under zero applied field 'on' state as function of temperature (x's). Plotted against Batdalov and Red'kos measured zero field thermal conductivity (circles), Duval et. al.'s zero field measured thermal conductivity (squares).

data points, which agree well with both our measured sample 1 1.8 T data and Duval et al.'s 3 T data [8]. Duval et al.'s [8] data have similar temperature dependence for 0.6 T and 3 T, and agrees with the temperature dependence of our measured data. Our measured data for sample 2 under an applied field of 1.8 T correlates well with Duval et al.'s [8] measured data under an applied field of 0.6 T. This suggests our sample 2 is less pure than that tested by Duval et al. [8], as a much higher magnetic field is required to achieve similarly low thermal conductivity. Batdalov and Red'ko's [2] 2 T data has a much lower thermal conductivity, and a stronger temperature dependence. Canavan et al. [3] measure a minimum RRR value of 7×10^3, with a stated purity of 99.995%. Our sample 1 has a measured purity of 99.999%, thus it may be inferred that it has an RRR that is above 7×10^3. Duval et al. [8] claim their sample has an RRR value of the order of 100–200, implying purity below that of Canavan et al.'s sample. Our sample 2 has a measured purity of 99.992%, but since a higher field (1.8 T) is required to achieve the same performance as Duval et al.'s sample under a 0.6 T field we can infer that Duval et al.'s sample has a higher purity. We would therefore expect sample 2 to have a lower RRR value than the sample of Duval et al. [8]. Batdalov and Red'ko [2] measure their RRR to be 1.55×10^5, implying exceptional purity which would explain their extremely high measured performance.

The zero field thermal conductivity strongly depends on purity. The measured zero field conductivities for our sample 1 is shown in Fig. 5, plotted against the equivalent measurements taken by Duval et al. [8] and Batdalov and Red'ko [2]. Lower purity implies more crystal defects and impurities which cause increased scattering of the heat carriers, and a lower zero field thermal conductivity. The Wiedemann–Franz law states the proportionality between the thermal and the electrical conductivity, σ_0. Thus, samples of higher purity will have a higher σ_0, hence a greater $\omega_c\tau$ for a given applied field B. As previously stated, a greater $\omega_c\tau$ implies a greater magnetoresistive effect. Duval et al.'s [8] lower purity sample will therefore need a higher field to have the same magnetoresistive effect as our sample 1, as is seen from Fig. 4. The same argument applies to our sample 2. A higher purity sample will have a greater magnetoresistive effect as seen in Batdalov and Red'ko's data [2]. In fact, Batdalov and Red'ko [2] measure exceptionally high values for the low temperature zero field thermal conductivity, 100 kW m^{-1} K^{-1} at 4.2 K and increasing with decreasing temperature. Duval et al. [8] measure the equivalent quantity to be 0.4 kW m^{-1} K^{-1} at 4.2 K, where we measure 48.3 kW m^{-1} K^{-1} at 4.26 K for our sample 1, both decreasing with temperature (Fig. 5).

Another important property in sample difference is the geometry, specifically, the crystal width. The width of crystal used by Canavan et al. [3] was identical to our sample, at 1.5 mm. Duval et al. [8] use crystals of width 0.5 mm, whereas Batdalov and Red'ko [2] use a crystal of diameter 4.3 mm. Batdalov and Red'ko [2] calculate the mean free path of electrons to be $d \approx 1.4$ mm at 4 K. Crystal widths comparable to, and smaller than d will cause the electron conductivity to be limited more by boundary scattering. We see zero field conductivity measurements highest in Batdalov and Red'ko's [2] data, followed by our sample 1, and lastly in the results of Duval et al. [8]. Canavan et al. [3] have not published their zero field conductivity measurements. The 4.3 mm crystal tested by Batdalov and Red'ko [2] will have less significant boundary scattering, hence a higher zero field electronic conductivity and a higher σ_0. The 0.5 mm crystal of Duval et al. [8] will have a far higher degree of boundary scattering, as its width is smaller than d. This implies a lower zero field electronic conductivity, σ_0. This, and the purity argument, provides an explanation of why Duvall et al.'s [8] sample has the poorest zero field conductivity. The effect of crystal width on σ_0 will inevitably affect $\omega_c\tau$, and hence the strength of field required to achieve the same magnetoresistive effect. This theory agrees well with the observed results, in much the same way as the previous purity argument.

5. Conclusions

The thermal conductivity of a tungsten magnetoresistive heat switch, for use in an ADR, has been measured in the temperature range 0.3–4 K under applied magnetic fields of 0 T ('on' state) and 1.8 T ('off' state) for two samples of different purity. The resulting measurements for sample 1, of 99.999% purity, were fit to an equation originating from semi-classical magnetoresistance theory (Eq. (6)). Although results from other authors [10] indicate a T^2 dependent lattice conductivity, a T^3 dependence cannot be ruled out from our data. It seems that for our samples, under an applied field of 1.8 T, the dominant heat transfer mechanism is still heat transport via electrons.

The lower purity sample, sample 2, has a purity of 99.992%. This sample has a higher 'off' state conductivity than sample 1. It has a

comparable 'off' state conductivity under 1.8 T applied field to Duval et al.'s sample under an applied field of 0.6 T. It seems that the third decimal point in percentage purity has a strong effect on the magnetoresistive effect and the performance as a heat switch.

The switching ratio at 1.5 K for our sample 1 is 1.75×10^4 and at 4.26 K it is 1.51×10^4. This indicates a reasonably stable switching ratio over the investigated temperature range. Based on the presented measurements we suggest that to maximise the switching ratio a highly pure sample of tungsten (>99.999%) is required, and optimising its dimensions to control the scattering mechanisms that limit the flow of heat.

References

[1] Bartlett J, Hardy G, Hepburn ID, Brockley-Blatt C, Coker P, Crofts E, et al. Improved performance of an engineering model cryogen free double adiabatic demagnetisation refrigerator, these Proceedings.
[2] Batdalov AB, Red'ko NA. Lattice and electronic thermal conductivities of pure tungsten at low temperatures. Sov Phys Solid State 1980;22(4):664–6.
[3] Canavan ER, Dipirro MJ, Jackson M, Panek J, Shirron PJ, Tuttle JG. In: Advances in cryogenic engineering: proceedings of the cryogenic engineering conference, vol. 47; 2002. p. 1183–90.
[4] Pippard AB. Magnetoresistance in metals (Cambridge studies in low temperature physics; 2). Cambridge: Cambridge University Press; 1989.
[5] Engels JML, Gorter FW, Miedema AR. Magnetoresistance of gallium – a practical heat switch at liquid helium temperatures. Cryogenics 1972;12(2):141–5.
[6] Laudy J, Knol A. A cadmium heat switch. Cryogenics 1966;6(6):370–1.
[7] Radebaugh R. Electrical and thermal magnetoconductivities of single-crystal beryllium at low temperatures and its use as a heat switch. J Low Temp Phys 1977;27:91–105.
[8] Duval JM, Cain BM, Timbie PT. Magnetoresistive heat switches and compact superconducting magnets for a miniature adiabatic demagnetization refrigerator. Cryocoolers, vol. 13. New York: Springer Science+Business Media, Inc.; 2004. p. 567–73.
[9] Long JR. Thermal and electrical transport in a tungsten crystal for strong magnetic fields and low temperatures. Phys Rev B 1971;3(4):1197–205.
[10] Wagner DK. Lattice thermal conductivity and high-field electrical and thermal magnetoconductivities of tungsten. Phys Rev B 1972;5(2):336–47.
[11] Lifshits IM, Azbel' MYa, Kaganov MI. Electron theory of metals. New York: Consultant's Bureau, New York (A Division of Plenum Publishing Corporation); 1973.
[12] Long JR. Lattice conductivity, Lorenz numbers, and Nernst-Ettingshausen effect in tungsten at liquid – helium temperatures. Phys Rev B 1971;3(8):2476–84.
[13] Wagner DK, Garland JC, Bowers R. Low-temperature electrical and thermal resistivities of tungsten. Phys Rev B 1971;3(10):3141–9.
[14] Fawcett E. Magnetoresistance of molybdenum and tungsten. Phys Rev 1962;128(1):154–60.
[15] Mateck GmbH. Im Langenbroich 20, D-52428 Juelich, Germany.